EPJ Web of Conferences **41**, 09013 (2013)
DOI: 10.1051/epjconf/20134109013

Strong-field photoemission from nanostructures driven by few-cycle mid-infrared fields

G. Herink, D. R. Solli, M. Gulde, and C. Ropers

Courant Research Center, University of Göttingen, Göttingen, Germany
Email: cropers@gwdg.de

Abstract. We present strong-field photoemission from plasmonic nanotips driven by ultrashort pulses at wavelengths of 0.8-8µm, reaching Keldysh parameters down to 0.1. We identify a sub-cycle acceleration regime that is exclusive to confined fields in nanostructures.

1 Introduction

Surfaces and nanostructures are increasingly becoming a subject of interest in strong-field physics [1-6]. Such dense systems allow for novel interactions and manipulation schemes of electron dynamics via the tailoring of materials and structures, resonances and field enhancements. Recently, the field enhancement at metallic nanotips was shown to result in localized above-threshold [3] and strong-field photoemission [4], including the observation of carrier-envelope effects [2]. However, using visible and near-infrared light frequencies, optical damage occurs close to the transition into the strong-field regime, which limits Keldysh parameters to values near unity and ponderomotive energies to the order of the work function.

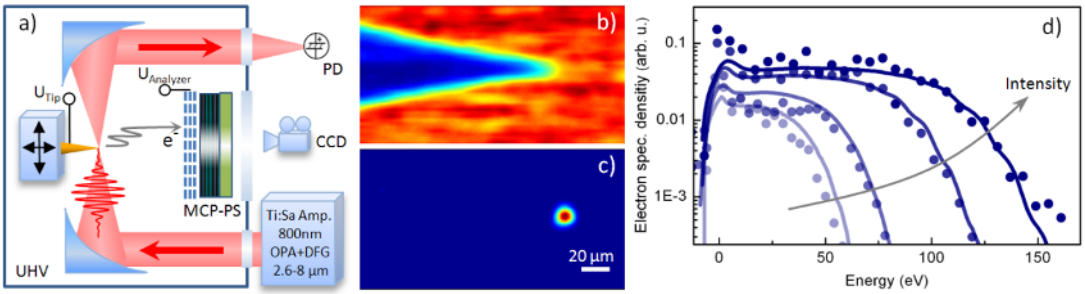

Fig. 1 a Experimental setup. Femtosecond pulses (wavelengths 0.8 – 8 µm) from a titanium:sapphire laser amplifier, an optical parametric amplifier and a difference frequency generation unit are focused onto a metal nanotip in ultrahigh vacuum (UHV). Shadow images of the tip (**b**) are recorded by raster scanning it in the focal plane, while the electron emission is recorded with a phosphor screen microchannel plate (MCP-PS) and a charge-coupled device (CCD) camera (**c**). The localized signal in c indicates emission exclusive to the apex (spot size given by focus diameter). Intensity dependent kinetic energy spectra (circles in **d**, shown for a wavelength 3.8 µm) are measured using a retarding field. Solid lines: Simulated spectra, incorporating locally enhanced, spatially inhomogeneous field.

Here, we deeply enter the strong-field regime by increasing the driving wavelength to the mid-infrared spectral range [6]. We demonstrate localized optical field emission at wavelengths between 800 nm and 8 μm, observing light-field induced electron acceleration above hundreds of eV. At high local intensities and long wavelengths, a sub-cycle acceleration regime is encountered, where electrons escape the nanolocalized near-fields within a fraction of an optical half-cycle [6].

2 Experiments, Results and Discussion

The experimental setup is shown in Fig. 1**a**. Ultrashort near- and mid-infrared pulses produced by difference frequency generation of signal and idler waves from an optical parametric amplifier are focused onto electrochemically etched gold nanotips (radii of curvature 10-20 nm). Shadow-images are acquired by scanning the tip in the focal plane and recording the transmitted light (Fig. 1**b**). In this raster scanning, a strong photoelectron signal is obtained at direct apex excitation only (Fig. 1**c**), demonstrating localized emission from the tip apex using ultrashort mid-infrared pulses (wavelength in Figs. 1**b**, **c**: 3.8 μm). Such localized photoemission was found at all wavelengths between 800 nm and 8 μm, evidencing the broadband nature of the field enhancement at such tips. The field-dependent electron yield (not shown) is consistent with the emission being induced by quasistatic tunnelling. Electron kinetic energy spectra (Fig. 1**d**) display a high energy plateau reaching beyond 100 eV. Both the plateau and the intensity-dependent cutoff are reproduced by simulations (solid lines in Fig. 1**d**) employing an adapted two-step photoemission model [7]. This Simpleman model includes adiabatic tunnel emission and, most importantly, the propagation and acceleration of electrons in the locally enhanced and spatially confined optical near-field at the tip apex.

The large optical bandwidth accessible in these measurements allows for studying the wavelength dependence of the field-driven electron dynamics near the nanostructures. From the scaling of the ponderomotive energy with frequency ($U_p=e^2F^2/4m\omega^2$, with m,e: electron mass and charge, ω: frequency, F: field amplitude), a quadratic increase of the cutoff energy with wavelength may be expected. However, our measurements show a strong deviation from this behaviour, caused by the spatial inhomogeneity of the driving field. Figure 2a shows the observed cutoff versus wavelength for two values of the local intensity (squares: 5.4TW/cm^2, triangles: 40TW/cm^2). We find that the cutoff strongly increases only for short wavelengths, displaying a much slower increase at longer wavelengths. The transition to the saturation region is characterized by a kind of spatial adiabaticity parameter δ, which we define as the ratio of the 1/e-field decay length l_F and the frequency- and field-dependent electron quiver amplitude: $\delta = l_F/l_q = l_F m\omega^2/eF$. The cutoff saturation corresponds to values of $\delta<1$, where the quiver amplitude exceeds the near-field decay length. In this regime, electrons leave the nanometric field-enhanced region within much less an optical half-cycle (cf. Fig. 2**b**). The transition to such conditions is accompanied by a decreasing importance of rescattering (cf. Fig. 2**a**). Alongside the changes in cutoff, the phase-dependence of the final kinetic energy of emitted electrons is drastically modified (Fig. 2**c**), with the phase of maximum energy shifted to later times.

In conclusion, we have studied ultrafast field-driven photoemission from sharp metal tips over a large spectral range. We find electron acceleration that is governed by the spatial inhomogeneity of the driving field in the optical hot-spot. These observations illustrate new degrees of freedom to manipulate and tailor electron dynamics in nanostructures and establish the utility of mid-infrared fields in exploring strong-field physics in such systems.

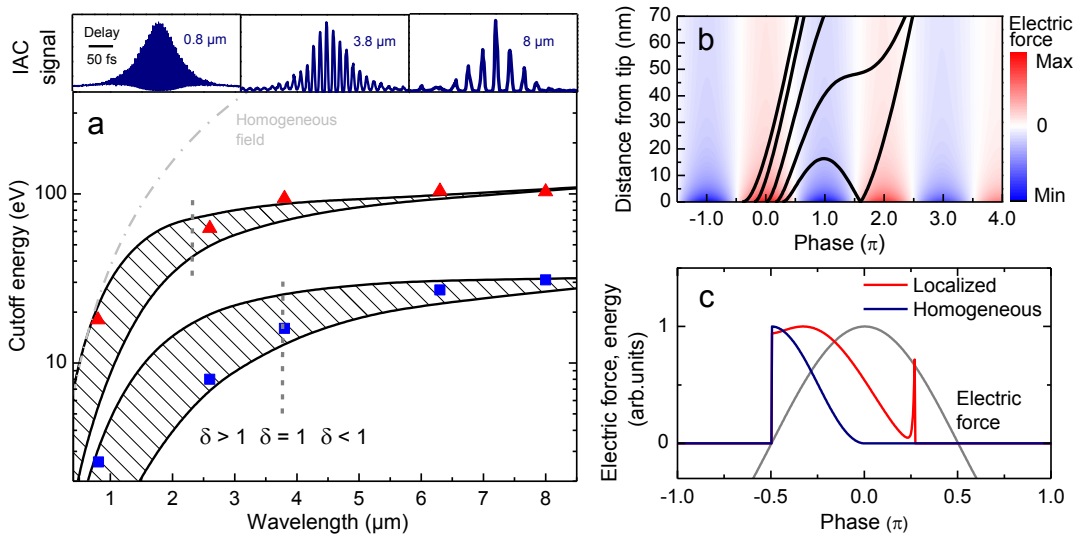

Fig. 2. a Experimentally observed scaling of the cutoff-energy with wavelength at two local intensities (triangles, squares). Solid lines: Simulations within adapted two-step model. Upper and lower bounds of the shaded corridors: Simulations with unity and zero reflection coefficient at surface, respectively. Dash-dotted line: Cutoff simulated for a spatially homogeneous field of equal intensity. A spatial adiabaticity parameter δ identifies the regime, in which the quiver amplitude exceeds the near-field decay length (δ<1). Insets: Interferometric autocorrelations, measured using the nonlinear electron emission signal. **b** Simulated electron trajectories for different emission phases (8 μm wavelength). The quiver motion is strongly influenced and partially suppressed by the near-field decay length. **c** Simulated final kinetic energies (normalized) of emitted electrons as a function of emission phase for homogeneous (blue) and localized (red) fields. Electric driving force (grey) at 8 μm wavelength. For localized fields, the phase of maximum kinetic energy shifts towards the maximum of the driving force. The final peak corresponds to acceleration from a subsequent optical cycle.

References

1. S. Zherebtsov *et al.*, Nat. Phys. **7**, 656 (2011)
2. M. Krüger, M. Schenk, P. Hommelhoff, Nature **475**, 78 (2011)
3. M. Schenk, M. Krüger, P. Hommelhoff, Phys. Rev. Lett. **105**, 257601 (2010)
4. R. Bormann, M. Gulde, A. Weismann, S. V. Yalunin, C. Ropers, Phys. Rev. Lett. **105**, 147601 (2010)
5. P. Rácz *et al.*, Appl. Phys. Lett. **98**, 111116 (2011)
6. G. Herink, D.R. Solli, M. Gulde, C. Ropers, Nature **483**, 190 (2012)
7. P. B. Corkum, Phys. Rev. Lett. **71**, 1994 (1993)